QUANTUM GASES

Pauli blocking of atom-light scattering

Christian Sanner*†, Lindsay Sonderhouse†, Ross B. Hutson, Lingfeng Yan, William R. Milner, Jun Ye*

Transition rates between coupled states in a quantum system depend on the density of available final states. The radiative decay of an excited atomic state has been suppressed by reducing the density of electromagnetic vacuum modes near the atomic transition. Likewise, reducing the density of available momentum modes of the atomic motion when it is embedded inside a Fermi sea will suppress spontaneous emission and photon scattering rates. Here we report the experimental demonstration of suppressed light scattering in a quantum degenerate Fermi gas. We systematically measured the dependence of the suppression factor on the temperature and Fermi energy of a strontium quantum gas and achieved suppression of scattering rates by up to a factor of 2 compared with a thermal gas.

Radiative relaxation of an excited quantum system is a ubiquitous phenomenon: it makes fireflies glow, underlies the radiative recombination of electrons and holes in light-emitting diodes, and can be observed as gamma decay of nuclear isomers. The intimately related phenomenon of light scattering involves minimally populated excited states that often assume a virtual character (*1*, *2*). The blue sky is a direct manifestation of such a second-order excitation-emission process, with air molecules scattering sunlight. What all these light–matter interactions have in common is that the radiative decay depends on the final density of states for the joint emitter-photon system. For the photon channel in particular, it has been demonstrated (*3*–*5*) that manipulation of the density of vacuum modes through the use of an electromagnetic resonator modifies the emission and scattering of light. This so-called Purcell effect is now widely used in nanostructured devices (*6*). More than 30 years ago, it was suggested (*7*) that constraints imposed by the quantum statistics of an atomic medium could also modify spontaneous emission and light scattering. Fermi statistics requires the total wave function of a fermionic system to be antisymmetric, giving rise to the Pauli exclusion principle, which forbids indistinguishable fermions from occupying the same internal and external quantum states. Accordingly, if a sufficient number of ground-state fermionic atoms occupy all available external motional states into which an internally excited fermionic atom has to decay, this decay process will be blocked. Reducing light-scattering rates and extending the natural lifetime of an excited atomic state by embedding it inside a Fermi sea has been the theme of many theoretical studies and proposals (*8*–*17*), but experimental observation has been complicated by atomic properties and competing collective radiative behavior.

JILA, National Institute of Standards and Technology and University of Colorado, Boulder, CO 80309, USA.
†These authors contributed equally to this work.
*Corresponding author. Email: christian.sanner@jila.colorado.edu (C.S.); ye@jila.colorado.edu (J.Y.)

Spontaneous emission and light scattering are not synonymous. Even though the usual descriptions (*2*) of both processes involve the relaxation of an excited state (a populated atomic energy eigenstate and a virtual intermediate state, respectively), their properties and decay dynamics are different. In a noninteracting Fermi gas, however, the unavailability of final momentum states is the sole cause for single-particle modifications of radiative (re)emission properties and therefore universally affects all atom-light processes that transfer randomly directed recoil momentum to the atom (*13*).

Here we report a direct observation of Pauli suppression of light scattering using a quantum degenerate Fermi gas of strontium atoms. We confirm that the suppression becomes stronger as degeneracy is increased and when the Fermi energy approaches the photon recoil energy. By angularly resolving the photon scattering rate, we measured up to a factor-of-two reduction of light scattering in comparison to the value determined from a thermal ensemble. This distinctive manifestation of Fermi statistics connects the fundamental radiative property of atoms to their motional degrees of freedom subject to quantum statistics. The consequences of Pauli blocking of atomic motion have been previously demonstrated, including the suppression of collisions (*18*), the direct observation of Fermi pressure (*19*), the onset of Hanbury Brown–Twiss anticorrelations (*20*, *21*), local antibunching (*22*–*24*), the suppression of chemical reactions between molecules (*25*), and the formation of Pauli crystals (*26*).

Figure 1 illustrates the key concept of the experiment and introduces the relevant energy scales (*27*). An ensemble of N harmonically confined identical, noninteracting fermions of mass m forms a quantum degenerate Fermi sea with near-unity occupation of the oscillator states if the thermal energy $k_B T$ is small compared with the Fermi energy $E_F = (6N)^{1/3}\hbar\omega$. The three-dimensional (3D) confinement is characterized by the mean trap frequency $\omega = (\omega_x\,\omega_y\,\omega_z)^{1/3}$, and k_B and $\hbar$ denote the Boltzmann and reduced Planck constants, respectively. The Fermi temperature T_F and Fermi wave vector k_F are defined via $E_F = (\hbar k_F)^2/(2m) = k_B T_F$. If an atom at rest inside the Fermi sea absorbs a photon carrying momentum $\hbar\boldsymbol{k}_{abs}$, it gains a corresponding recoil energy $E_R = (\hbar\boldsymbol{k}_{abs})^2/2m$. Here, we consider the case of weak confinement with $\hbar\omega \ll E_R$ and treat Rayleigh scattering as a two-step momentum transfer process (*14*, *28*). Upon photon reemission, the atom experiences a randomly directed second momentum kick $\hbar\boldsymbol{k}_{emi}$, where $|\boldsymbol{k}_{emi}| = |\boldsymbol{k}_{abs}| = k_R$, resulting in a total momentum transfer $\hbar\boldsymbol{k} = \hbar\boldsymbol{k}_{abs} + \hbar\boldsymbol{k}_{emi}$. If, however, the corresponding motional state is already occupied by another atom within the Fermi sea, this decay channel is blocked, and light scattering will be suppressed. The relative temperature T/T_F and the wave vector ratio k/k_F, where $\hbar k_F = (2mE_F)^{1/2}$ is the momentum space radius of the Fermi sea, determine the density of available final momentum states and hence the degree of blockade. Following Fermi's golden rule, one finds, using a local density approach (*11*, *14*), a relative scattering rate of

$$S(\boldsymbol{k}) = \frac{\int d^3\boldsymbol{p}\, d^3\boldsymbol{q}\, n_i(\boldsymbol{p},\boldsymbol{q})[1 - n_f(\boldsymbol{p},\boldsymbol{q})]}{\int d^3\boldsymbol{p}\, d^3\boldsymbol{q}\, n_i(\boldsymbol{p},\boldsymbol{q})}$$

Here the integrals cover the six-dimensional phase space spanned by three momentum dimensions $\boldsymbol{p}$ and three real-space dimensions $\boldsymbol{q}$. The initial and final state phase space cell occupations are given by $n_i = n_{FD}(\boldsymbol{p}, \boldsymbol{q})$ and $n_f = n_{FD}(\boldsymbol{p}+\hbar\boldsymbol{k}, \boldsymbol{q})$, where n_{FD} is the Fermi-Dirac distribution for a harmonically trapped ideal Fermi gas, that is

$$n_{FD}(\boldsymbol{p},\boldsymbol{q}) = \frac{1}{1 + \xi^{-1}\exp\left[\left\{\sum_i p_i^2/(2m) + \sum_i m\omega_i^2 q_i^2/2\right\}/k_B T\right]}$$

The index i runs over all three dimensions, and ξ is the fugacity related to T/T_F via $1/\mathrm{Li}_3(-\xi) = -6(T/T_F)^3$, where Li_3 is the trilogarithm function. The expression for $S(\boldsymbol{k})$ counts all available final momentum states for a given momentum transfer $\hbar\boldsymbol{k}$ and averages over all initial states within the Fermi sea.

The above analysis suggests two pathways to observe pronounced Pauli suppression of light scattering. One can either prepare a Fermi gas with $E_F \gg E_R$ so that a substantial blockade is obtained for all emission directions, that is, for any momentum transfer up to the maximum $2\hbar k_R$ (homogeneously colored right sphere in Fig. 1C). Or one can relax this requirement and selectively observe only scattering events with a small momentum transfer so that $E_F \sim E_R$ is sufficient. The second approach, which we took in this study (gradient-colored left sphere in

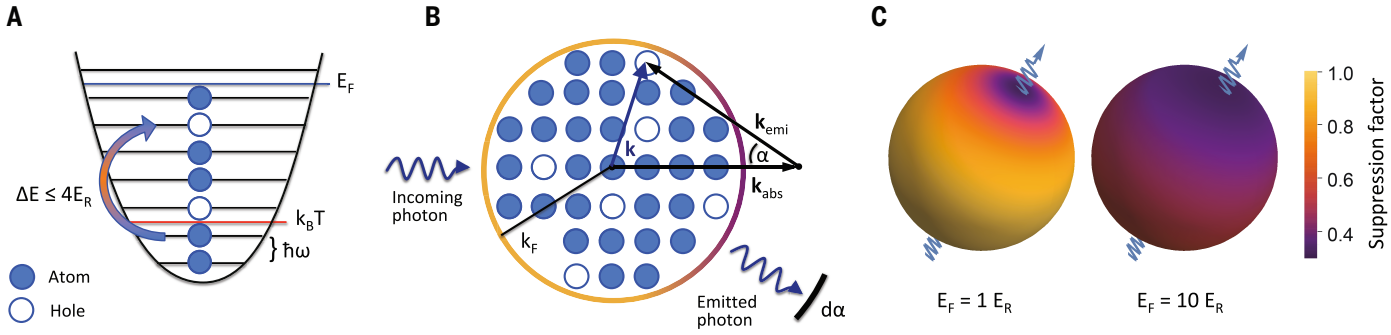

Fig. 1. Light scattering on atoms embedded inside a Fermi sea. (**A**) Indistinguishable fermions obey the Pauli exclusion principle. If the thermal energy $k_B T$ is sufficiently low, they fill almost all available harmonic oscillator states up to the Fermi energy E_F with near-unity occupation. When scattering a photon, the atom's motional energy can change by up to four times the recoil energy E_R. (**B**) In momentum space, the atoms form a Fermi sea occupying most states up to the Fermi momentum $\hbar k_F$. Light scattering with reemission along α and total momentum transfer $\hbar \boldsymbol{k}$ can happen only if the final momentum state is not occupied by another ground-state fermion. Here, the atom initially in the center of the Fermi sea is assumed to scatter a photon. Atoms closer to the Fermi surface can reach a higher number of unoccupied momentum states. A detector covering a solid angle $d\alpha$ registers the emitted photon. (**C**) Pauli blocking leads to a characteristic angular distribution of scattered photons in the deeply degenerate regime (here, $T/T_F = 0.1$). For $E_F \sim E_R$ (left sphere), scattering is preferentially suppressed in a small cone around the forward direction, whereas $E_F \gg E_R$ (right sphere) causes strong suppression for all scattering angles α. The suppression factor specifies the scattering rate relative to a non-Pauli-blocked sample.

Fig. 1C), is straightforwardly realized in a small-angle light scattering configuration where a small number of atoms in the Fermi sea are optically excited, and a subset of the scattered photons is collected under a shallow angle α with respect to the excitation beam corresponding to a momentum transfer of $\hbar k = 2\hbar k_R \sin(\alpha/2)$.

A multitude of effects besides quantum statistics can influence radiation dynamics in a dense ensemble of emitters. Coherence, either externally imprinted or spontaneously established, can lead to super- and subradiant collective states that correspondingly exhibit super- and subnatural radiative lifetimes. Dicke superradiance (*29*, *30*), radiation trapping (*31*), multiple scattering (*32*), and other forms of coherent or incoherent collective scattering (*33*) all critically depend on the integrated optical density $\mathrm{OD} = \int \sigma n \, dl$ of the atomic gas. This attenuation parameter, derived from the single-atom scattering cross section σ and density n, where length l is measured along the direction of the incoming light, defines a parameter region where the gas is optically thin ($\mathrm{OD} \ll 1$) and single-particle scattering dominates over collective effects. Given that on resonance, σ is on the order of the squared optical wavelength $\lambda^2 = (2\pi/k_R)^2$, and k_F is tied to the 3D peak density via $n = k_F^3/6\pi^2$, it is not possible to satisfy the Pauli blocking criterion $k_F \sim k_R$ without violating the small OD requirement. Indeed, typical optical densities encountered in atomic Fermi gas experiments easily exceed 100. In this optically thick regime, multiple photon scattering strongly affects the light propagation inside the sample, as evidenced by the resonant fluorescence image displayed in Fig. 2B. Using off-resonant light reduces the effective scattering cross section and renders the atom cloud weakly absorbing for the incoming probe light at sufficient detuning. This, combined with differential observation strategies and avoiding light detection in the forward direction, minimizes the influence of collective scattering dynamics. Furthermore, unlike Pauli blocking, these competing effects are not dependent on quantum statistics and can therefore be observed using a thermal gas (*34*), instead of a quantum degenerate gas, to provide a baseline.

Our experiment started with the preparation of a ^{87}Sr Fermi gas, as previously described (*35*). The $^1S_0$ $F = 9/2$ ground state is split into 10 magnetic spin states $m_F = -9/2, \ldots, 9/2$. Here, F is the total angular momentum of the nuclear spin. This fully thermalized 10-component sample (*36*) contains 18,000 atoms per spin state confined in a crossed optical dipole trap with maximum radial trap frequencies of $\omega_x = \omega_y = 2\pi \times 120$ Hz and an axial confinement with $\omega_z = 2\pi \times 506$ Hz. This leads to a Fermi energy of $E_F = 440$ nK for each of the 10 Fermi seas; we reached temperatures down to $0.1\ T_F$. The small intercomponent s-wave scattering length $a = 97 a_0$, where a_0 is the Bohr radius, makes the Fermi gas weakly interacting, with $k_F a = 0.06$, which is scaled by the number of spin states, increasing the total energy of the gas by <7% compared with a noninteracting gas. These weak repulsive interactions in principle affect $S(\boldsymbol{k})$, but their differential effect on temperature measurements and scattering rates is negligible (*36*) at the measurement precision achieved in this study. Under suitable conditions, any optical excitation returning to the ground state should experience a decay blockade. We performed specific measurements on the $^1S_0$-$^1P_1$ transition at 461 nm with a natural linewidth (*37*) of $\Gamma = 2\pi \times 30.4$ MHz and a recoil energy of $E_R = 520$ nK. Using a continuous weak-drive Rayleigh scattering scheme, the Fermi gas was exposed for 1 μs to a 1.2-GHz detuned drive beam that causes, on average, <10% of the atoms to undergo an excitation cycle. No evidence for inelastic scattering was observed.

For the given drive beam and atom cloud parameters, the sample was optically thin with an effective OD of 0.02, corresponding to a forward transmission of 98%. As illustrated in Fig. 2, two detectors collected scattered photons simultaneously under off-axis angles of $\alpha_1 = 24°$ and $\alpha_2 = 72°$. These operational parameters were chosen to simplify the interpretation of our measurements. First, as discussed above, the detuning from resonance by 40Γ eliminates multiple scattering dynamics and furthermore avoids refractive lensing contributions (*38*) far off-axis. Second, the low excitation rate keeps the Fermi sea intact throughout the probe pulse exposure. Third, operating in the weak-drive limit ensures that there is no inelastic scattering contribution beyond the recoil-induced energy shift, i.e., Mollow triple-peaked fluorescence spectra and other strong-drive effects are negligible (*2*).

To systematically explore how quantum degeneracy affects light scattering, we started with a deeply degenerate gas of $T/T_F = 0.1$ and gradually heated it up to $T/T_F = 0.7$ through parametric confinement modulation while keeping the atom number and Fermi energy constant. Under these conditions, photons scattered off of the weak probe pulse were counted. To satisfy the requirement to minimally disturb the Fermi gas by the probe, the number of collected photons along the two

detection axes was correspondingly low. Even for the axis with a high numerical aperture (NA) of 0.23, fewer than 200 photons were collected at full quantum efficiency. By operating the gated CCD detectors in a hardware binning mode that maps all detected photons onto a 3 by 3 superpixel array, we spatially and temporally isolated the signal from background contributions and maintained low readout noise. The measured photon counts were compatible with ab initio estimates (*38*) within 30%, on the basis of the reported drive parameters and detection efficiencies. All relevant thermodynamic parameters were independently assessed through measurements on expanded gas clouds after time of flight.

The results of Pauli-suppressed scattering are shown in Fig. 3A. Under the shallow off-axis angle of 24°, where $k/k_F = 0.45$ for our Fermi sea, we find a strong dependence of the photon counts on T/T_F. To properly normalize the detector signal, that is, to convert the registered photon counts to a suppression ratio without introducing an arbitrary scaling factor, it was necessary to prepare an equivalent reference sample that was not Pauli-blocked. Because the weak optical confinement did not maintain a constant atom number for $T/T_F > 1$, we devised an alternative method to eliminate Pauli blocking: At 10 μs before applying the actual probe pulse, we exposed the Fermi gas to a 5-μs-long pre-pulse that destroyed the Fermi sea by randomly exciting atoms to momentum states beyond k_F. Consequently, light scattering was no longer Pauli-suppressed during the subsequent probe pulse. All round blue data points in Fig. 3, A and B, are normalized to a common reference photon count obtained from a single pre-pulse–exposed sample, as detailed in (*39*). Numerically integrating the expression for $S(\boldsymbol{k})$ at all probed temperatures reveals good agreement between experiment and theory. The simultaneously acquired measurements at an observation angle of 72° do not show a pronounced suppression and only exhibit a weak temperature dependence, as expected for $k/k_F = 1.27$, as most final momentum states lie outside of the Fermi sea.

To further verify that Pauli blocking is the mechanism responsible for the observed scattering behavior, we studied the dependence of the suppression factor on k_F/k_R by varying the confinement while keeping the atom number and $T/T_F = 0.13$ constant, as displayed in Fig. 3B. Even at the shallowest confinement with $k_F/k_R = 0.57$ ($E_F/E_R = 0.32$), the momentum transfer along the 24° axis amounted to only $k/k_F = 0.74$, so that we still observed substantial suppression of light scattering. This is in contrast to the 72° case, where $k/k_F = 2.07$ at $k_F/k_R = 0.57$. If $k/k_F > 2$, Pauli blocking is negligible at any temperature, so we normalized all photon counts acquired under 72° (red data points in Fig. 3, A and B) with respect to this reference point (solid red circle in Fig. 3B).

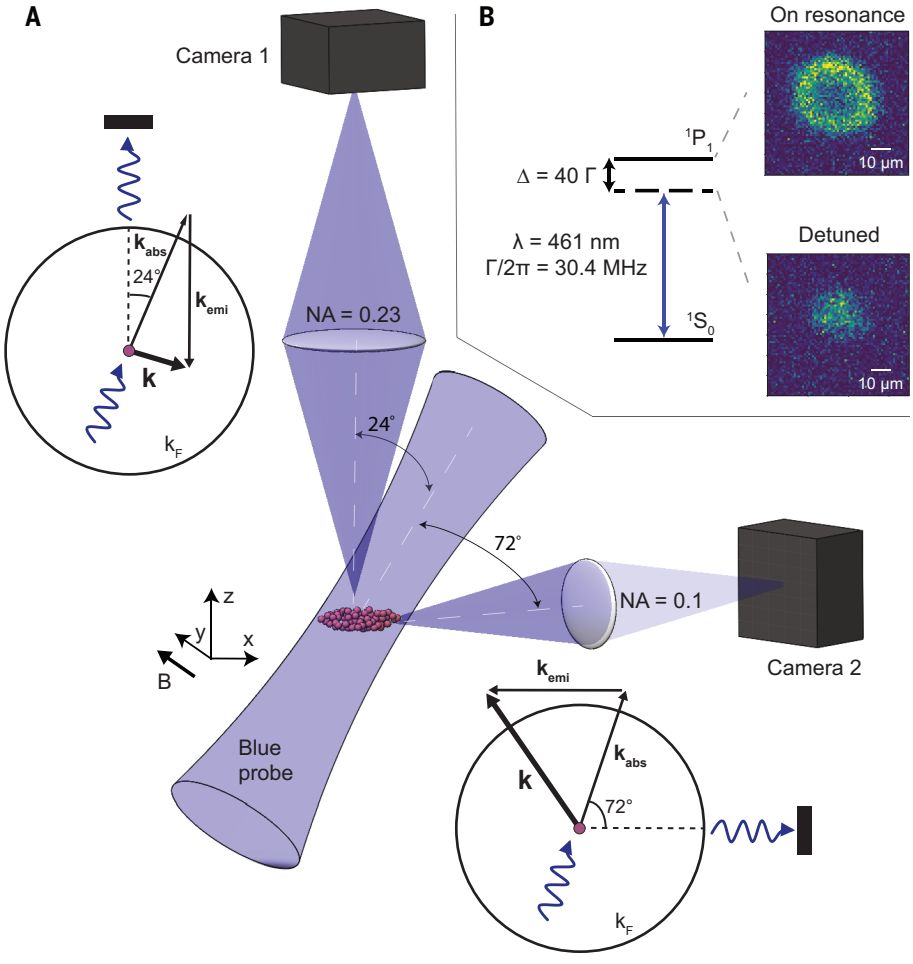

Fig. 2. Experimental setup. (**A**) Off-resonant probe light excites ^{87}Sr atoms inside a Fermi sea. Scattered photons are collected simultaneously along two imaging axes under angles of 24° and 72°, with their numerical apertures (NA) shown. Small scattering angles correspond to a small momentum transfer with $k/k_F < 1$, whereas the transversal observation detects photons from scattering events with $k/k_F > 1$. The circularly polarized probe beam has an intensity of 5 I_{sat}, where the resonant saturation intensity is $I_{sat} = 41$ mW/cm^2. (**B**) On resonance, the atomic cloud is optically thick for the probe beam, and the image formed on camera 1 displays a hole in the cloud center owing to multiple scattering. At a detuning of $\Delta = 40\Gamma$, the atom cloud is optically thin, and the corresponding image resembles the atomic density distribution. The detuned frequency is used in the Pauli blocking experiment. A magnetic bias field of 3 G applied in the horizontal plane along the *y* direction defines the atomic quantization axis.

The additional, blue square data points displayed in Fig. 3 were normalized by applying a pre-pulse separately for each data point and are in good agreement with the common-mode normalized measurements. In particular, with a 10-μs wait time before the probe pulse, the atomic density remains essentially the same with or without the pre-pulse. This ensures common-mode cancellation of collective scattering dynamics. In fig. S1, we present light scattering measurements with variable pre-pulse durations for a deeply degenerate ($T/T_F = 0.11$) and heated ($T/T_F = 0.58$) Fermi gas. These data confirm the scattering-induced destruction of the Fermi sea over the course of the pre-pulse application.

Spatially resolving the origin of the scattered photons within the Fermi gas, in addition to counting the total number of scattered photons along a given direction, provides a visual revelation of the Pauli blocking mechanism. For this purpose, we modified the 24° high-NA axis to deliver magnified images of the atom cloud and used a nonbinning CMOS camera with a low readout noise of two photoelectrons. The cylindrically symmetric

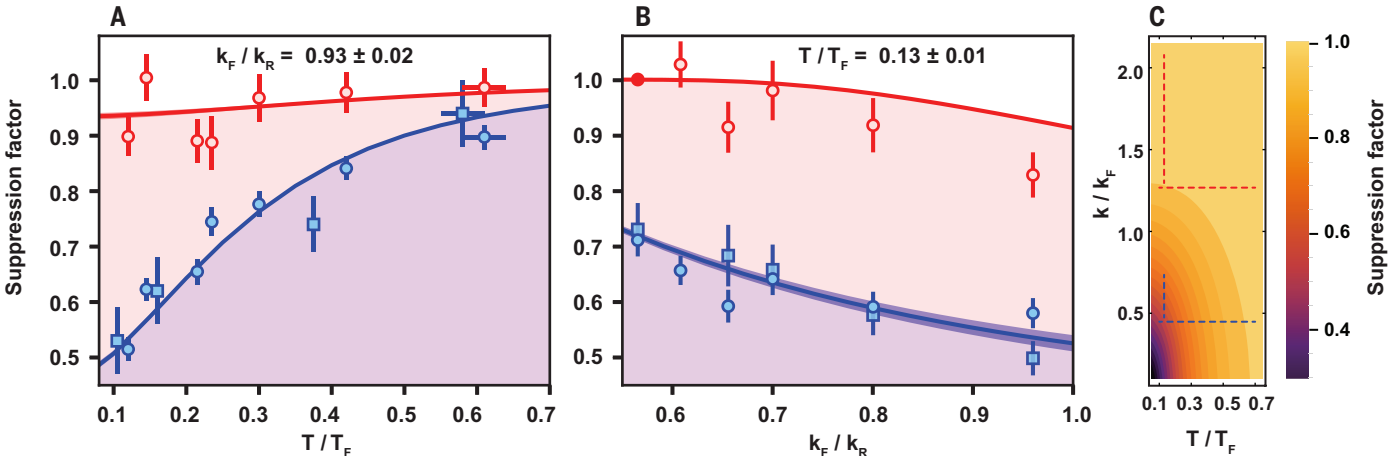

Fig. 3. Suppression of light scattering in a ^{87}Sr Fermi gas over a range of temperatures and Fermi momentums. All measurements are performed with a 10-component Fermi gas containing 18,000 atoms per spin state. The scattering behavior is distinctly different for the two observation angles of 24° (blue circles and squares) and 72° (red circles). Raw photon counts are normalized with respect to measurements on non-Pauli-blocked reference samples (see text). Each circle data point is derived from 150 iterations of the experiment, and each square point results from 50 experimental runs. Solid theory curves are calculated with no free parameters (*14*). The widths of the theory lines reflect the experimental uncertainties of Fermi energy and temperature. The error bars are purely statistical and indicate one-standard-deviation confidence intervals. (**A**) At a constant Fermi wave vector of $k_F/k_R = 0.93$ ($E_F/E_R = 0.86$), the atom ensemble's scattering cross section decreases as the gas approaches deep quantum degeneracy with decreasing temperature. The suppression observed under 24° is pronounced, and the suppression factor reaches 50% at $T/T_F = 0.13$. In contrast, under 72°, the suppression is negligible. (**B**) At constant $T/T_F = 0.13$, k_F is varied by adiabatically changing the confinement. A larger k_F results in a stronger suppression. (**C**) The data reported in (A) and (B) are measured along four trajectories (dashed lines) through the parameter space spanned by k/k_F and T/T_F. Depending on the scattering angle, k varies between 0 and $2k_R$. Light collected under an off-axis angle of 24° corresponds to a momentum transfer $\hbar k < \hbar k_F$ for the given Fermi gas, leading to substantial reduction of the density of available final states. In contrast, for the 72° collection angle, the corresponding momentum transfer $\hbar k > \hbar k_F$. Thus most final states are not blocked, and scattering is not suppressed.

atomic cloud at $T/T_F = 0.12$ with a diameter of ~20 μm was projected along the z axis into a 2D image with 0.9-μm-wide pixels. Because a single pixel collects, on average, less than one photon, it is necessary to average hundreds of frames in order to derive a finely resolved scattering profile. Furthermore, we azimuthally averaged the mean image to obtain the radial profile (blue data points) shown in Fig. 4. Residual optomechanical drifts in the optical setup caused small displacements of the center of mass position of the cloud during the frame averaging period. This, together with the finite resolution of the imaging system, led to an effective $1/e^2$ pixel blurring on the order of 3 μm. To compare the observed scattering profile against theory predictions without introducing a free scaling parameter, we independently acquired in situ profiles of the Fermi gas through the same imaging setup via high-intensity fluorescent imaging (*40*). In this high-intensity limit, the light scattering rate is saturated and Pauli suppression effects are eliminated. Peak column density and width of these in situ profiles agree well with calculated atomic density distributions. Assuming no Pauli blockade, the scattering profiles at high and low probe intensities will therefore be related by a single rescaling factor that is given as the ratio of the total photon counts measured in the two cases. The so derived scattering profile expected without Pauli blockade for the weak probe beam is represented by the purple curve in Fig. 4. Momentum space integration plus one-dimensional line-of-sight integration of $S(\boldsymbol{k})$ yields a radially resolved suppression ratio for us to then determine the expected scattering profile with Pauli blockade (blue curve in Fig. 4). Except at the center of the cloud, where radial averaging does not substantially improve the signal-to-noise ratio, we find good agreement between calculated and measured profiles. Toward the outer rim of the cloud, the local Fermi energy drops so that light scattering is not suppressed anymore; the local suppression ratio will approach the thermal gas limit of 1. This happens, as seen with the blue theory curve, only in the outermost region, where the density is so low that the signal-to-noise level is insufficient to reliably determine a suppression ratio.

We have reported here a clear demonstration that Fermi statistics leads to strongly modified light scattering in a quantum degenerate system. The presence of a Fermi sea alters the final atomic motional mode spectrum and enables a direct observation of Pauli blockade of light scattering. Interpreted from a many-body system perspective, this experiment probes the structure factor (*41*) of a quantum degenerate Fermi gas. Defined as the Fourier transform of the spatial density–density correlation, the static structure factor $S(\boldsymbol{k})$ characterizes the linear response of a system to a perturbation with wave vector $\boldsymbol{k}$. Accordingly, the suppression of light scattering and the suppression of density fluctuations (*23*) in a Fermi gas are

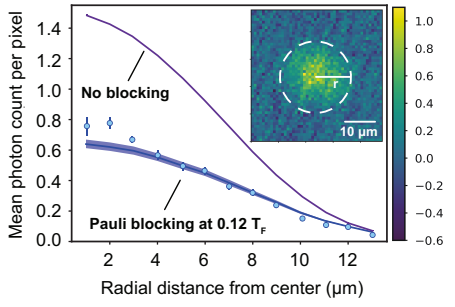

Fig. 4. Spatially resolved light scattering from a trapped Fermi gas at $T/T_F = 0.12$. Azimuthally averaging the spatially resolved mean photon count (inset) from 1100 individual images obtained along the z axis yields a radial light scattering profile (blue data points). In situ column density images, separately obtained using a high-intensity fluorescent imaging technique, are used to predict the scattering signal for a nondegenerate gas (purple curve). The spatial profile of light scattering calculated for the $T/T_F = 0.12$ ensemble (blue curve) agrees well with the measured data.

two interrelated manifestations of the same fundamental many-body physics.

Beyond the regime of Rayleigh scattering, we envision directly measuring a prolonged excited state lifetime using properly prepared quantum states (*42*). The capability of altering a fundamental decoherence mechanism will contribute to the quantum engineering of atom–light interfaces. In particular, custom-designed Fermi reservoirs can protect optical qubits at local nodes while facilitating cavity-free directional photon emission for efficient network connectivity. In the context of optical atomic clocks, this work could enable spectroscopic interrogation times exceeding the natural lifetime of the excited clock state and investigation of previously unexplored radiative properties of atoms.

REFERENCES AND NOTES

1. J. J. Sakurai, *Advanced Quantum Mechanics* (Addison-Wesley, 1967).
2. R. Loudon, *The Quantum Theory of Light* (Oxford Univ. Press, ed. 3, 2000).
3. E. M. Purcell, *Phys. Rev.* **69**, 681 (1946).
4. D. Kleppner, *Phys. Rev. Lett.* **47**, 233–236 (1981).
5. R. G. Hulet, E. S. Hilfer, D. Kleppner, *Phys. Rev. Lett.* **55**, 2137–2140 (1985).
6. L. Novotny, B. Hecht, *Principles of Nano-Optics* (Cambridge Univ. Press, 2006).
7. K. Helmerson, M. Xiao, D. E. Pritchard, in *International Quantum Electronics Conference*, A. Owyoung, C. Shank, S. Chu, E. Ippen, Eds., vol. 8 of OSA Technical Digest (Optical Society of America, 1990), paper QTHH4.
8. A. Imamoglu, L. You, *Phys. Rev. A* **50**, 2642–2645 (1994).
9. J. Javanainen, J. Ruostekoski, *Phys. Rev. A* **52**, 3033–3046 (1995).
10. T. Busch, J. R. Anglin, J. I. Cirac, P. Zoller, *Europhys. Lett.* **44**, 1–6 (1998).
11. B. DeMarco, D. S. Jin, *Phys. Rev. A* **58**, R4267–R4270 (1998).
12. J. Ruostekoski, J. Javanainen, *Phys. Rev. Lett.* **82**, 4741–4744 (1999).
13. A. Görlitz, A. P. Chikkatur, W. Ketterle, *Phys. Rev. A* **63**, 041601 (2001).
14. B. Shuve, J. H. Thywissen, *J. Phys. At. Mol. Opt. Phys.* **43**, 015301 (2009).
15. R. M. Sandner, M. Müller, A. J. Daley, P. Zoller, *Phys. Rev. A* **84**, 043825 (2011).
16. R. Onofrio, *Phys. Rev. A* **93**, 033414 (2016).
17. A. Piñeiro Orioli, A. M. Rey, *Phys. Rev. Lett.* **123**, 223601 (2019).
18. B. DeMarco, S. B. Papp, D. S. Jin, *Phys. Rev. Lett.* **86**, 5409–5412 (2001).
19. A. G. Truscott, K. E. Strecker, W. I. McAlexander, G. B. Partridge, R. G. Hulet, *Science* **291**, 2570–2572 (2001).
20. T. Rom *et al*., *Nature* **444**, 733–736 (2006).
21. T. Jeltes *et al*., *Nature* **445**, 402–405 (2007).
22. T. Müller *et al*., *Phys. Rev. Lett.* **105**, 040401 (2010).
23. C. Sanner *et al*., *Phys. Rev. Lett.* **105**, 040402 (2010).
24. A. Omran *et al*., *Phys. Rev. Lett.* **115**, 263001 (2015).
25. L. De Marco *et al*., *Science* **363**, 853–856 (2019).
26. M. Holten *et al*., *Phys. Rev. Lett.* **126**, 020401 (2021).
27. S. Giorgini, L. P. Pitaevskii, S. Stringari, *Rev. Mod. Phys.* **80**, 1215–1274 (2008).
28. A. P. Vinogradov *et al*., *Opt. Express* **29**, 2501–2520 (2021).
29. R. H. Dicke, *Phys. Rev.* **93**, 99–110 (1954).
30. M. Gross, S. Haroche, *Phys. Rep.* **93**, 301–396 (1982).
31. P. Weiss, M. O. Araújo, R. Kaiser, W. Guerin, *New J. Phys.* **20**, 063024 (2018).
32. M. C. W. van Rossum, T. M. Nieuwenhuizen, *Rev. Mod. Phys.* **71**, 313–371 (1999).
33. W. Guerin, M. T. Rouabah, R. Kaiser, *J. Mod. Opt.* **64**, 895–907 (2017).
34. S. L. Bromley *et al*., *Nat. Commun.* **7**, 11039 (2016).
35. A. Goban *et al*., *Nature* **563**, 369–373 (2018).
36. L. Sonderhouse *et al*., *Nat. Phys.* **16**, 1216–1221 (2020).
37. A. Heinz *et al*., *Phys. Rev. Lett.* **124**, 203201 (2020).
38. W. Ketterle, D. S. Durfee, D. M. Stamper-Kurn, in *Proceedings of the International School of Physics "Enrico Fermi,"* M. Inguscio, S. Stringari, C. E. Wieman, Eds. (IOS Press, 1999).
39. Materials and methods are available as supplementary materials.
40. M. T. DePue, S. Lukman Winoto, D. J. Han, D. S. Weiss, *Opt. Commun.* **180**, 73–79 (2000).
41. D. Pines, P. Nozieres, *The Theory of Quantum Liquids, Volume 1* (Addison-Wesley, 1988).
42. T. Bilitewski *et al*., arXiv:2108.02819 [cond-mat.quant-gas] (2021).
43. C. Sanner, Replication Data for: Pauli blocking of atom-light scattering, version 3, Harvard Dataverse (2021); https://doi.org/10.7910/DVN/LHUKWV.

ACKNOWLEDGMENTS

We thank P. Zoller, A. M. Rey, J. Thompson, and M. Holland for stimulating discussions and careful reading of the manuscript. **Funding:** Funding for this work was provided by the Defense Advanced Research Projects Agency, Air Force Office of Scientific Research, NSF Quantum Leap Challenge Institutes Office of Multidisciplinary Activities–2016244, NSF Phys-1734006, and National Institute of Standards and Technology. C.S. thanks the Humboldt Foundation for support. **Author contributions:** All authors contributed to carrying out the experiments, interpreting the results, and writing the manuscript. **Competing interests:** The authors declare that they have no competing financial interests. **Data and materials availability:** Data from the main text and supplementary materials are available through the Harvard Dataverse (*43*).

SUPPLEMENTARY MATERIALS

science.org/doi/10.1126/science.abh3483
Supplementary Text
Fig. S1

3 March 2021; accepted 1 October 2021
10.1126/science.abh3483

Pauli blocking of atom-light scattering

Christian SannerLindsay SonderhouseRoss B. HutsonLingfeng YanWilliam R. MilnerJun Ye

Science, 374 (6570), • DOI: 10.1126/science.abh3483

Photons not welcome

Two identical fermions cannot occupy the same quantum state, or so says the Pauli principle. For a cold gas of fermionic atoms, this means that all states up to the Fermi energy will be occupied, with only the atoms with the highest energy able to change their state. Such conditions have long been predicted to suppress light scattering off gases because the atoms receiving a kick from collisions with photons would have no state to move to. Deb *et al*., Margalit *et al*., and Sanner *et al*. now describe this so-called Pauli blocking of light scattering. —JS